Telemetry Monitoring System with Features Explaining Anomalies Based on Mahalanobis Distance

Shun Katsube[1] and Hironori Sahara[2]

[1,2]*Tokyo Metropolitan University, Department of Aeronautics and Astronautics, Hino, Tokyo, 191-0065, Japan*
katsube-shun@ed.tmu.ac.jp
sahara@tmu.ac.jp

ABSTRACT

Because satellites cannot be repaired once launched, operators must detect anomalies early and prevent failures before they occur. Thus, satellite telemetry monitoring systems need to alert operators of anomalies and provide them with useful information to deal with these anomalies. However, traditional knowledge-based monitoring systems have the challenges of difficulty in building comprehensive models and a high dependency on experts. In recent years, data-driven approaches have been actively studied with the development of machine learning algorithms. These approaches solve the challenges of knowledge-based methods; however, they are often less capable of explaining anomalies than knowledge-based methods. In this study, we propose the new telemetry monitoring system with feature engineering to explain anomalies. The proposed method realizes identifiability of anomaly types and unusual telemetry by designing features based on moving averages, telemetry periods, waveform differences, and the Mahalanobis distance. We applied the proposed features to artificial and practical abnormal datasets and evaluated their usefulness. The results showed that the proposed method is capable of identifying trend, periodic, and waveform anomalies, specifying the telemetry in which the anomaly occurred and providing the information to operators.

1. INTRODUCTION

Although developing satellites requires significant time, manpower, and budget, satellite operators are physically unable to repair launched satellites. Thus, satellite operators constantly monitor telemetry data to detect anomalies as early as possible and prevent serious failures that could affect the continuation of operations. However, it is very labor-intensive for operators to manually identify the causes of anomalies from the huge amount of telemetry. Given these backgrounds, telemetry monitoring systems must provide operators with additional information about anomalies in association with alerting them to these anomalies.

The mainstream of telemetry monitoring systems are knowledge-based approaches. Limit checking, in which a threshold is set for each telemetry, is often used because it is easy for humans to understand. Other methods are rule-based (Mizutani et al, 2009) and model-based (Williams & Nayak, 1996), where diagnostic rules and physical models are designed in advance. However, constructing appropriate thresholds and comprehensive diagnostic rules for complex satellite systems is highly time-consuming and labor-intensive. Moreover, there are problems with the possibility of missing unknown anomalies and the high dependence on skilled operators.

With the recent development of machine learning algorithms, data-driven health monitoring systems have been researched and developed. Data-driven methods reduce the effort of constructing models and dependence on experts, because anomaly detection models are constructed inductively using historical data instead of expert knowledge in these methods. In general, anomaly detection models are built from normal data using unsupervised learning methods owing to the difficulty of obtaining anomaly data before training the models (Yairi et al., 2021). That is, any data that deviate from usual behavior are considered anomaly data; therefore, the models have the potential to detect anomalies that are not known by operators. Data-driven methods in satellites often use predictive modeling approaches because satellites are dynamical systems and telemetry is time-series data. Time-series prediction algorithms, such as long short-term memory, are used to forecast future telemetry values, and anomaly scores are determined by prediction accuracy (Chen et al., 2021; Hundman et al., 2018; Tariq et al., 2019; Wu et al., 2020). Other approaches focus on feature representations and use autoencoders (Sakurada & Yairi, 2014), principal component analysis (Barreyre et al., 2019; Xiong et al., 2011; Yairi et al., 2017), and dictionary

https://doi.org/10.36001/IJPHM.2024.v15i2.3945

learning (Pilastre et al., 2020). In these approaches, anomaly scores are computed as reconstruction errors or distances from normal behavior in the feature space.

As described above, data-driven methods solve the problems of knowledge-based methods. However, in many cases, the models constructed by unsupervised learning only output anomaly scores and cannot contribute to the identification of unusual telemetry and anomaly types necessary for operators to deal with abnormalities. This lack of explainability has been discussed in recent years in satellites (Yairi et al., 2021) and other fields, and Yepmo et al. (2022) state that anomalies are explained by feature importance, feature values, data points comparison, and structure analysis.

Hence, this study aims to develop a telemetry monitoring system that can explain anomalies based on feature engineering. In the context of telemetry monitoring, Barreyre et al. (2019) have focused on feature engineering and designed features using fixed functional bases and principal component analysis. However, their method does not consider anomaly explanations, and it is necessary to construct a model for each telemetry to specify abnormal telemetry. In this study, we target periodic time-series telemetry and propose the feature representation that can identify anomaly types and unusual telemetry. First, the feature vectors corresponding to each anomaly type are extracted from the telemetry using the moving average, periodogram, and Kullback–Leibler (KL) divergence. Then, those feature vectors are summarized into a three-dimensional feature vector and anomaly score by two times Mahalanobis distance (MD) calculation. In operation, when anomaly is detected by monitoring the anomaly score, the proposed method suggests the type of anomaly and abnormal telemetry by calculating the contribution of each feature vector variation. The contributions of this study can be summarized as follows:

- We classified anomalies occurring in periodic time-series telemetry into trend, periodic, and waveform anomalies. Then, we designed the feature representation that can identify the anomaly types and unusual telemetry based on this classification.
- We applied the proposed method to artificial abnormal datasets and practical anomaly events, demonstrating that it can provide operators with the information they need to deal with anomalies.
- The proposed method contributes to realizing a telemetry monitoring system that reduces operator effort by providing additional information about anomalies as well as warnings by anomaly scores.

The rest of this paper is composed of the following sections: Section 2 categorizes anomalies based on previous studies; Section 3 defines the proposal method; Section 4 presents the results of applying the proposed method to the abnormal datasets and discusses them; and Section 5 provides the conclusion and future perspectives.

2. ANOMALY CLASSIFICATION

As with conventional knowledge-based approaches, it is difficult to exhaustively enumerate anomalies occurring on satellites. Thus, based on anomaly types mentioned or verified in previous studies, we classify anomalies into three categories: trend, periodic, and waveform. This classification is not specific fault names such as thermal runaway, bus voltage drops, or incorrect attitude controls. Even so, when trend anomalies are observed in temperature telemetry, operators can assume the occurrence of thermal runaway based on this information.

In the field of anomaly detection, the mainstream anomaly categories are point, group, and contextual anomalies (Ruff et al., 2021), which are also mentioned in the context of telemetry monitoring (Hundman et al., 2018; Pilastre et al., 2020; Tariq et al., 2019; Wu et al., 2020; Xiong et al., 2011). First, point anomalies are basically described as spikes of a single data point, but they are also considered a series of out-of-range anomalies (Pilastre et al., 2020). In addition, Yairi et al. (2017) state that outliers are often trivial anomalies occurring temporarily as a result of data conversion or transmission errors and should be distinguished from truly serious anomalies. Thus, we do not consider point anomalies such as spike values, as outliers are removed by the preprocessing described in Section 4.2. Next, group and contextual anomalies are summarized as time-dependent group anomalies (Hundman et al., 2018; Tariq et al., 2019) or categorized as periodicity anomalies (Figure 1a) and pattern anomalies (Figure 1b) (Barreyre et

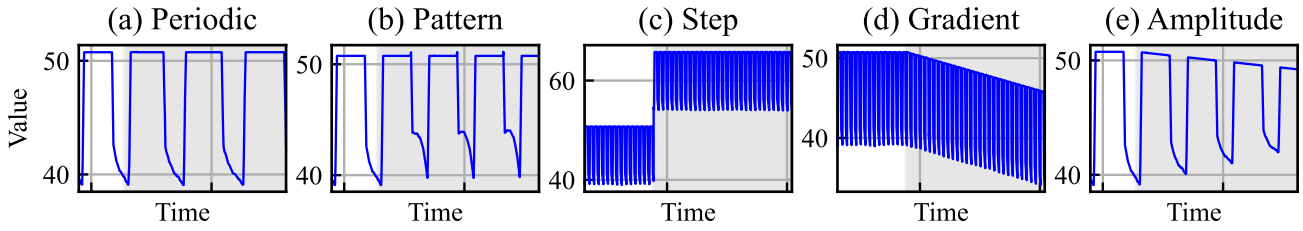

Figure 1. Types of anomalies. The gray background indicates abnormal time. In this study, (a) is classified as periodic anomalies, (b) and (e) as waveform anomalies, and (c) and (d) as trend anomalies.

al., 2019) because the telemetry is periodic time-series data. As these types of anomalies occur within normal value ranges, operators may miss them by simply monitoring raw telemetry with limit checking. Other classifications include the mathematical fault models by Cui et al. (2023): pulsed anomaly, step-type anomaly (Figure 1c), gradient anomaly (Figure 1d), and periodic anomaly. Of these classifications, step-type and gradient anomalies are time-dependent group anomalies that focus on the trend of the telemetry, rather than on the period and waveform.

Based on the above, we classify time-dependent group anomalies into trend, periodic, and waveform anomalies. First, trend anomalies are cases in which the trend of telemetry fluctuation changes significantly. They include step-type anomalies, gradient anomalies, and series of out-of-range anomalies in the previous categories. In practical operation, they occur in temperature and voltage telemetry in the event of thermal runaway or a drop in generated voltage.

Next, periodic anomalies are cases in which the period of telemetry changes and may occur within the normal value range. Periodicity of telemetry that depends on the satellite's orbital period, such as battery voltage and surface temperature, rarely changes, and satellites are likely to have a serious failure at the time it changes. However, the telemetry of mission equipment that is routinely used by operators can cause this type of anomaly.

Lastly, waveform anomalies are cases in which telemetry does not show the expected waveform or the telemetry amplitude changes (Figure 1e). These types of anomalies can occur in a wide range of telemetry owing to equipment failure or changes in component characteristics.

3. PROPOSED METHOD

3.1. Feature Extraction

Figure 2 shows the workflow of the proposed method. Initially, the moving average, period, and distribution difference are extracted from the telemetry as the features corresponding to the anomaly classification in Section 2. Subsequently, we summarize those features into a single feature vector using the two times MD calculation and compute the anomaly score. This feature extraction is performed for each telemetry series of length W. In this study, we let W be the length of 1 day's telemetry for simplicity. Thus, the series of telemetry processed at time t is $\mathbf{X}_m^{(t)} = \left[x_m^{(t-W+1)}, \dots, x_m^{(t)}\right]$, where $x_m^{(\cdot)}$ is the observed value and $m = 1, \dots, M$ is the label of telemetry.

First, a simple way to represent a trend of telemetry is the moving average. More robust methods for outliers include the moving median and moving trimmed average. However, we use the moving average because these robust methods are slower to respond to changes in trend, and outliers are removed by the preprocessing in Section 4.2. Thus, the trend feature is expressed by Eq. (1) with $\mathcal{J} = \{t - W + 1, \dots, t\}$ as the set of time steps. Here, if this feature has a constant value and its variance is zero, the MD cannot be calculated in Section 3.2, so we add to the average a random number generated from a normal distribution with a sufficiently small variance and the zero mean. In this study, the random number is $\epsilon^{(t)} \sim N(0, 0.001)$, and this is added for the remaining features as well.

$$y_{\mathrm{MA},m}^{(t)} = \frac{1}{W}\sum_{j\in\mathcal{J}} x_m^{(j)} + \epsilon^{(t)} \tag{1}$$

Next, we estimate the telemetry period using the periodogram. The periodogram is a method of estimating the power spectral density (PSD) in signal processing, and

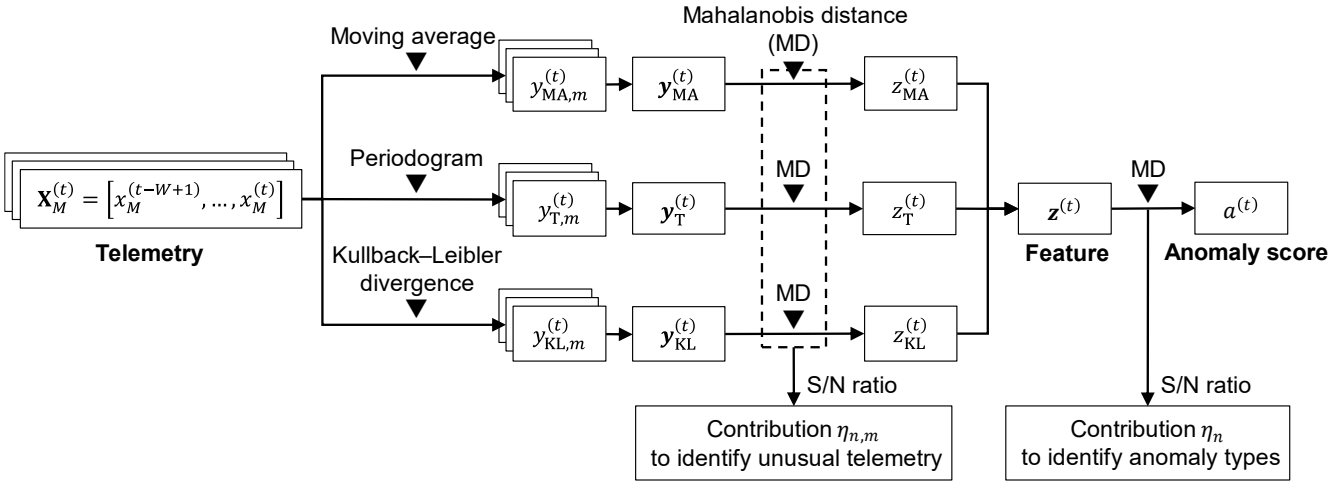

Figure 2. Flow of the proposal method.

the estimated PSD is obtained by $S_k^{(t)} = \left|f_k\left(\mathbf{X}_m^{(t)}\right)\right|^2/W$ using the discrete Fourier transform $f_k\left(\mathbf{X}_m^{(t)}\right) = \sum_{j=t-W+1}^{t} w^{(j)} x_m^{(j)} e^{-i2\pi kj/W}$. Here, $w^{(j)}$ is a window function, which, in this study, is the Hann window. Then, the period feature is represented by Eq. (2) using k where $S_k^{(t)}$ has the peak value. Δt is the sampling period of the telemetry.

$$y_{\mathrm{T},m}^{(t)} = \frac{W\Delta t}{k} + \epsilon^{(t)} \tag{2}$$

Lastly, we use the KL divergence between $\mathbf{X}_m^{(t)}$ and $\mathbf{X}_m^{(t-W/2)}$ distributions as the waveform feature. Although there are distance-based methods for calculating waveform differences, we calculate distribution differences to obtain only the waveform change without the influence of period and average changes. Thus, let $p_t(\cdot)$ and $p_{t-W/2}(\cdot)$ be the probability distributions of $\mathbf{X}_m^{(t)}$ and $\mathbf{X}_m^{(t-W/2)}$, respectively, and the waveform feature is given by Eq. (3).

$$y_{\mathrm{KL},m}^{(t)} = \sum_{j\in\mathcal{J}} p_t\left(x_m^{(j)}\right) \log \frac{p_t\left(x_m^{(j)}\right)}{p_{t-W/2}\left(x_m^{(j-W/2)}\right)} + \epsilon^{(t)} \tag{3}$$

3.2. Feature Summarization

We denote by Eq. (4) the new feature vector consisting of the features defined in Section 3.1, where $n = \mathrm{MA}, \mathrm{T}, \mathrm{KL}$ is the label of the feature.

$$\boldsymbol{y}_n^{(t)} = \left[y_{n,1}^{(t)}, y_{n,2}^{(t)}, \ldots, y_{n,m}^{(t)}, \ldots, y_{n,M}^{(t)}\right]^{\top} \tag{4}$$

We then summarize the feature vector using the MD from the usual vectors. In the field of quality management, outlier detection using the MD from normal datasets, called the unit space, is widely used as the Mahalanobis–Taguchi system (MTS) (Woodall et al., 2003). Although the MTS is a classical method, it is still evolving as improved methods are proposed currently (Mota-Gutiérrez et al., 2018). In addition, the MTS has the advantage of aggregating data into one-dimensional distances, considering correlations between data, and calculating the contribution to increasing distances by the signal-to-noise (S/N) ratio.

The summarized feature computed by the MD is expressed in Eq. (5), and the proposed feature vector is given by Eq. (6). Here, $\bar{\boldsymbol{y}}_n^{(t)}$ and $\boldsymbol{\Sigma}_n^{(t)}$ are the mean vector and covariance matrix of $\boldsymbol{y}_n^{(\cdot)}$, respectively.

$$z_n^{(t)} = \frac{1}{M}\left(\boldsymbol{y}_n^{(t)} - \bar{\boldsymbol{y}}_n^{(t)}\right)^{\top} {\boldsymbol{\Sigma}_n^{(t)}}^{-1} \left(\boldsymbol{y}_n^{(t)} - \bar{\boldsymbol{y}}_n^{(t)}\right) \tag{5}$$

$$\boldsymbol{z}^{(t)} = \left[z_{\mathrm{MA}}^{(t)}, z_{\mathrm{T}}^{(t)}, z_{\mathrm{KL}}^{(t)}\right]^{\top} \tag{6}$$

In actual operation, satellites cannot store all telemetry and can only send some telemetry to the ground station owing to communication limitations. Thus, anomaly detection should be performed on board, requiring that the parameters be updated incrementally. In this study, $\bar{\boldsymbol{y}}_n^{(t)}$ and $\boldsymbol{\Sigma}_n^{(t)}$ are updated by Eqs. (7) and (8), respectively, where it is necessary to give initial values, such as estimates from telemetry at the initial operation. In addition, the telemetry at time steps judged to be abnormal by the anomaly score described in Section 3.3 is not used in the update to prevent degradation of the estimated values.

$$\bar{\boldsymbol{y}}_n^{(t)} = \bar{\boldsymbol{y}}_n^{(t-1)} + \frac{\boldsymbol{y}_n^{(t)} - \bar{\boldsymbol{y}}_n^{(t-1)}}{t} \tag{7}$$

$$\boldsymbol{\Sigma}_n^{(t)} = \frac{(t-1)}{t}\boldsymbol{\Sigma}_n^{(t-1)} + \frac{1}{t}\left(\boldsymbol{y}_n^{(t)} - \bar{\boldsymbol{y}}_n^{(t-1)}\right)\left(\boldsymbol{y}_n^{(t)} - \bar{\boldsymbol{y}}_n^{(t)}\right)^{\top} \tag{8}$$

3.3. Anomaly Score

We define the anomaly score by computing the MD from the set of normal $\boldsymbol{z}^{(\cdot)}$ to $\boldsymbol{z}^{(t)}$, as shown in Eq. (9). Here, $\bar{\boldsymbol{z}}^{(t)}$ and $\boldsymbol{\Sigma}_{\mathrm{z}}^{(t)}$ are the mean vector and covariance matrix of $\boldsymbol{z}^{(\cdot)}$, respectively, which are updated as in Section 3.2. Abnormalities are judged by limit checking using a threshold of anomaly score a_{th}.

$$a^{(t)} = \frac{1}{3}\left(\boldsymbol{z}^{(t)} - \bar{\boldsymbol{z}}^{(t)}\right)^{\top} {\boldsymbol{\Sigma}_z^{(t)}}^{-1} \left(\boldsymbol{z}^{(t)} - \bar{\boldsymbol{z}}^{(t)}\right) \tag{9}$$

3.4. Contribution Calculation

In the MTS, the S/N ratio is used empirically as a measure of the data's usefulness for outlier detection. Typically, this measure is used to select data for use in the MTS, where it compares cases of inclusion and exclusion of data in the MD calculation (Woodall et al., 2003).

In this study, we compute the contribution of each component of $\boldsymbol{y}_n^{(\cdot)}$ to $z_n^{(\cdot)}$ using the S/N ratio as in Eq. (10), where $\mathcal{J}_a$ is the set of abnormal time steps; $y_{n,m}^{(j)}$ and $\bar{y}_{n,m}^{(j)}$ are the m component of $\boldsymbol{y}_n^{(j)}$ and $\bar{\boldsymbol{y}}_n^{(j)}$, respectively; and ${\sigma_{n,m}^2}^{(j)}$ is the (m,m) component of $\boldsymbol{\Sigma}_n^{(j)}$. Because $\eta_{n,m}$ increases as $y_{n,m}^{(j)}$ deviates from the usual, the component with relatively large $\eta_{n,m}$ among all components is likely to contribute to the abnormal events. The contribution of $z_n^{(\cdot)}$ to $a^{(\cdot)}$ is calculated in the same way.

$$\eta_{n,m} = -10\log\left[\sum_{j\in\mathcal{J}_a} \frac{{\sigma_{n,m}^2}^{(j)}}{\left(y_{n,m}^{(j)} - \bar{y}_{n,m}^{(j)}\right)^2}\right] \tag{10}$$

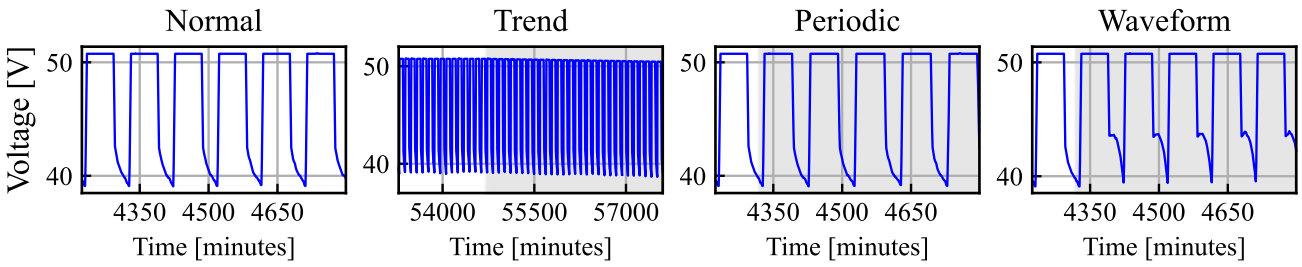

Figure 3. Normal telemetry and abnormal telemetry with reproduced anomalies. The gray background indicates abnormal time.

4. EXPERIMENTAL RESULTS

4.1. Setup

We applied the proposed method to the telemetry of the satellite Suzaku (ASTRO-EII), which is available online (https://darts.isas.jaxa.jp/astro/suzaku/). We targeted for experiments the voltage, current, and temperature telemetry labeled "DIST" (power distribution) and "HCE" (heater control electronics), which control power and temperature critical to the satellite's operational life. Then, we selected the continuous telemetry with confirmed periodicity to compose the five datasets shown in Table 1. Of these datasets, the trend, periodic, and waveform datasets are artificial abnormal cases that were made anomalies during the last 2 days by processing the telemetry of the normal dataset.

- **Normal:** This dataset consists of telemetry from August 25, 2005, to September 29, 2005, just after the start of Suzaku operations.
- **Trend:** The trend anomaly is reproduced by a linear decrease of 0.3 in the value of DIST_PCU_BUS_VOL_CAL over 2 days.
- **Periodic:** The periodic anomaly is reproduced by switching the period of "DIST_PCU_BUS_VOL_CAL" from 96 to 100 min, and then the period linearly increases to 110 min over 2 days.
- **Waveform:** The waveform anomaly is reproduced by cyclically adding a convex quadratic function $f(x) = -ax^2 + a, (-1 \leq x \leq 1)$ to the series of "DIST_PCU_BUS_VOL_CAL." The coefficient a increases linearly from 3 to 5 over 2 days.
- **Practical:** This dataset consists of telemetry from September 1, 2011, to January 24, 2012. Because this dataset includes a long operational period, we removed the telemetry related to mission equipment that fluctuates nonperiodically, and focused on bus equipment. Moreover, SAFEHOLD occurred at 1:27 a.m. on January 24, 2012, during Suzaku's operation, which is considered to be caused by an irregularity in the power system equipment (Umezu et al., 2019).

Dataset label	Number of telemetry	Number of samples
Normal	71	50400
Trend	71	50400
Periodic	71	50400
Waveform	71	50400
Practical	59	208888

Table 1. List of datasets

By comparing the results of the normal, trend, periodic, and waveform datasets, we confirmed that the proposed method is able to identify anomaly types and unusual telemetry. We also confirmed on the practical dataset that the proposed method can provide operators with useful information for detecting and dealing with practical anomaly events.

4.2. Preprocessing and Parameters

We preprocessed the telemetry before validation. First, the sampling period (Δt in Eq. 2) of all telemetry was resampled to 1 min to handle all telemetry values at each time step. Then, outliers were removed by a moving trimmed average. Because a large window size may smooth out the original telemetry waveforms, we eliminated the largest and smallest values with a window size of 5.

The proposed method requires several parameters. As already mentioned, the window size for the feature calculation is $W = 1440$ (1 day), and the sampling period is $\Delta t = 1$ min. The initial values of the covariance matrix $\boldsymbol{\Sigma}_n^{(0)}$ and mean vector $\bar{\boldsymbol{y}}_n^{(0)}$ in Eqs. 7 and 8 is calculated from the first 30-day portion of each dataset and is updated incrementally in subsequent time steps.

In addition, a threshold a_{th} is required for the anomaly score to detect anomalies via limit checking. If we had a sufficient amount of abnormal telemetry samples, we could determine an optimal threshold by considering the trade-off between false positives and false negatives. However, this was impossible in this study because we only know a limited number of anomaly events on Suzaku, similar to many other satellites. Thus, we a posteriori determined

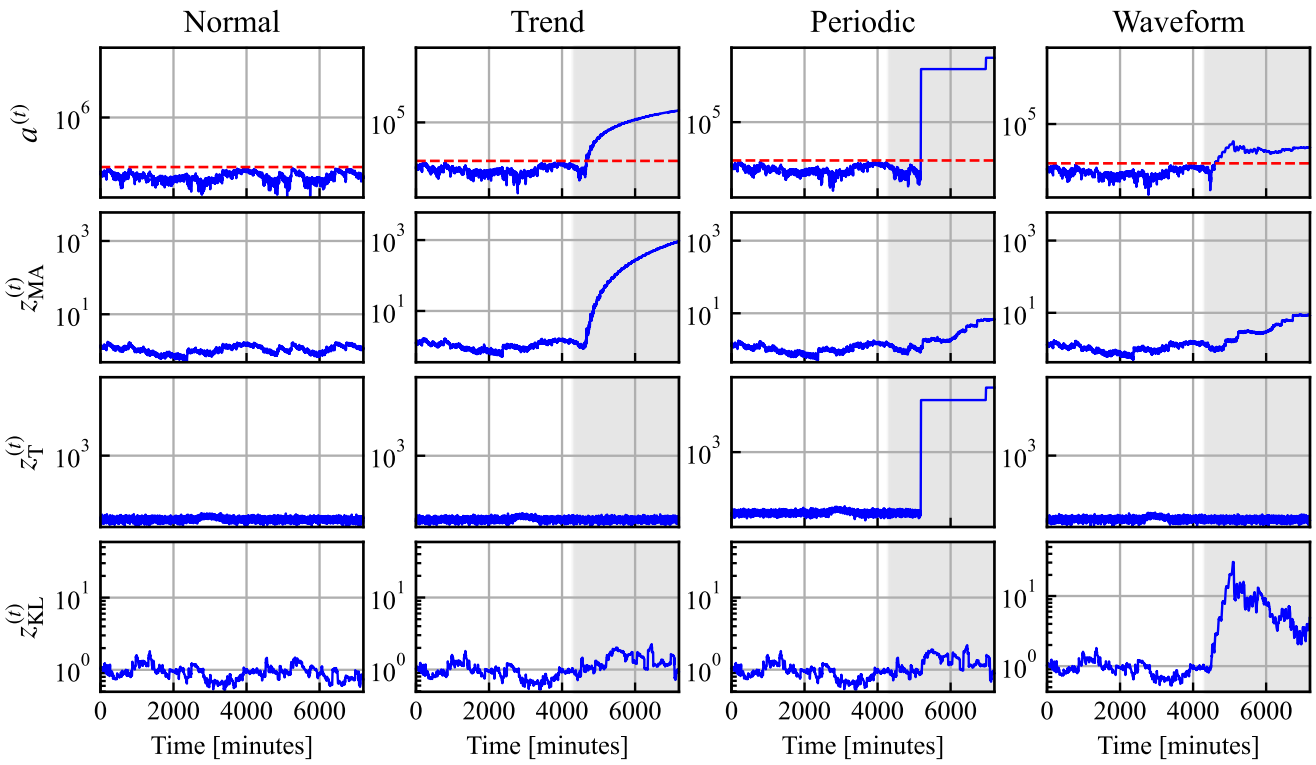

Figure 4. Anomaly scores and the components of feature vector for the last 5 days of the normal, trend, periodic, and waveform datasets shown on logarithmic axis. The red dotted line indicates the threshold $a_{th} = 2.5$, and the gray background indicates abnormal time.

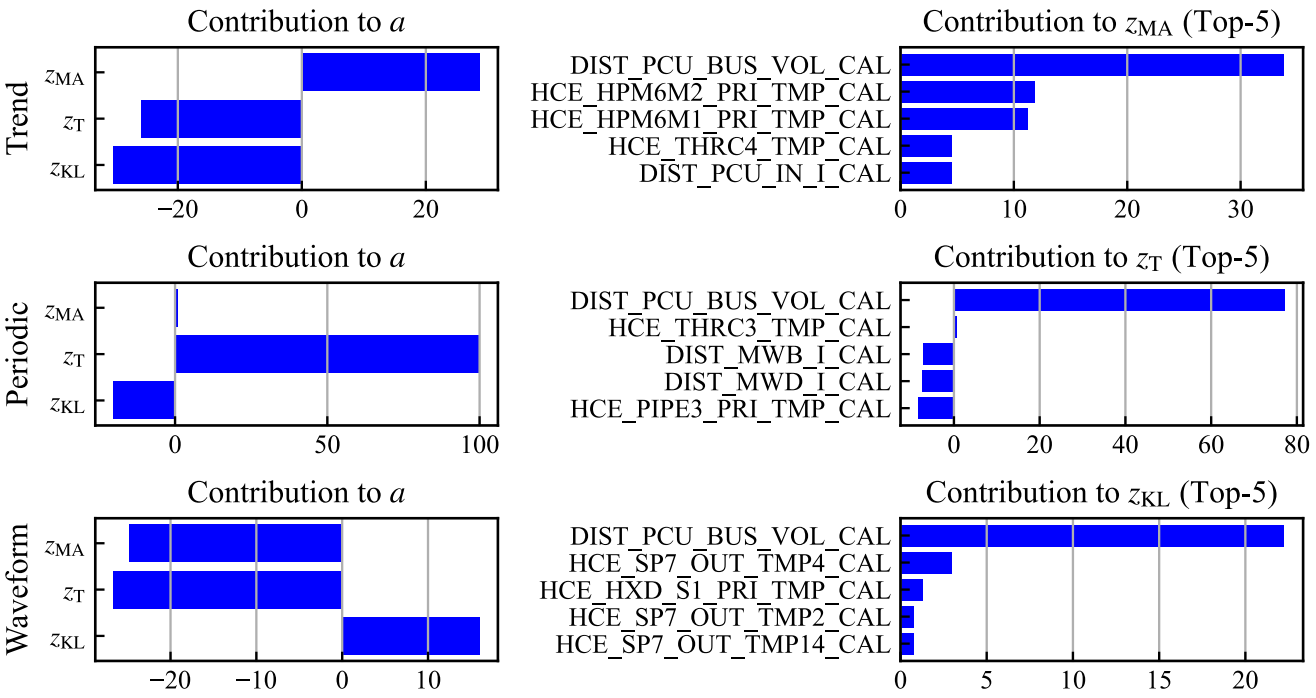

Figure 5. Contributions η to the anomaly scores and the components of feature vector.

appropriate thresholds to one decimal place of precision, which we set to $a_{th} = 2.5$ for the normal, trend, cycle, and waveform datasets and to $a_{th} = 34.2$ for the practical dataset.

4.3. Anomaly Score and Feature Vector Behavior

The first line of Figure 4 shows the anomaly scores calculated from the last 5 days of the normal, trend, periodic, and waveform datasets. The anomaly scores for the abnormal datasets rapidly increase and converge to a value higher than the threshold during the abnormal term, indicating that the proposed method is able to detect the anomalies. All anomalies were detected with a delay of 8 to 14 h from the start of the abnormal term. This delay is the number of time steps until the abnormal values occupy a sufficient proportion of the window length W to affect the estimated value. To reduce these delays, it is effective to decrease the window size in which features are calculated at each time step. However, smaller window sizes increase sensitivity to telemetry variations, potentially resulting in more false alarms. Thus, it is necessary to consider how much delay the satellite system can accept in operations.

The second to fourth rows in Figure 4 show the components of the feature vector. The components corresponding to anomalies in each dataset are increasing, showing that the proposed feature vector behaves differently depending on the anomaly type. However, z_{MA} in the periodic and waveform datasets, where no trend anomaly occurs, increased more than in the normal dataset. This difference in z_{MA} behavior is due to the fact that the telemetry values at the abnormal time steps in the periodic and waveform datasets are not used in the parameter update. In this study, all telemetry values at the abnormal time steps were eliminated from the updating, but a more detailed adoption rule for training data, such as eliminating only the values of telemetry with high contribution to anomaly, can construct a telemetry monitoring system that adapts to telemetry fluctuations more flexibly.

4.4. Identifying Anomaly Types and Anomaly Telemetry

The left column of Figure 5 shows the contribution of the components to the anomaly score in the trend, periodic, and waveform datasets. As was evident in the feature behavior in Figure 4, the contribution of the component corresponding to the anomaly that occurred in each dataset was the highest. Thus, the contribution using the S/N ratio can be used to identify the type of anomaly.

The right column of Figure 5 shows the top five contributions of telemetry to the component with the highest contribution. In all datasets, the contribution of "DIST_PCU_BUS_VOL_CAL," which is processed to reproduce the anomaly, has the highest value. These results show that the contribution can indicate the unusual telemetry in addition to the type of anomaly.

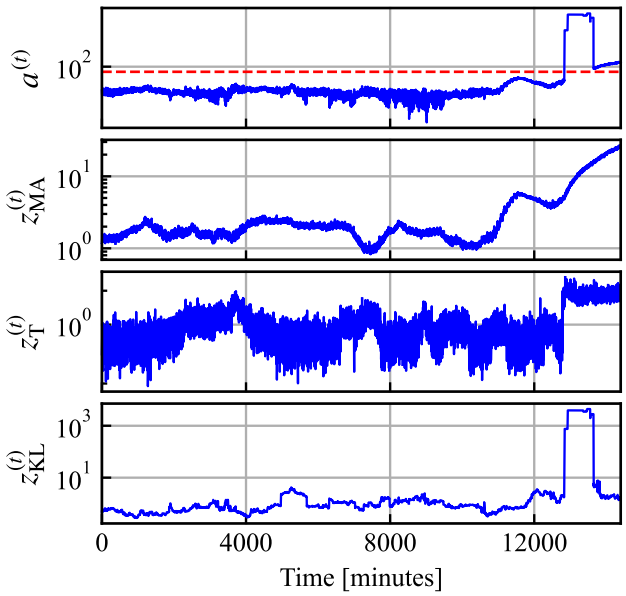

Figure 6. Anomaly score and the components of the feature vector for the last 10 days of the practical datasets shown on the logarithmic axis. The red dotted line indicates the threshold $a_{th} = 34.2$.

4.5. Practical Abnormal Event

The first row of Figure 6 shows the anomaly score calculated from the last 10 days of the practical dataset. The anomaly was detected 26 h before the last time step when SAFEHOLD occurred. Comparing this result with the results of Umezu et al. (2019) detecting the same event, the proposed method is faster than using a k-nearest neighbor and an autoencoder (13 and 12 h before, respectively) and slower than using a recurrent neural network and a one-class support vector machine (28 and 44 h before, respectively). Focusing on how the anomaly score increases, we can see first the rectangular increase, followed by the gradient increase. As the remaining rows of Figure 6 show, the rectangular and gradient increases were influenced by variations in z_{KL} and z_{MA}.

Figure 7 shows the contribution of the rectangular increasing part, and as expected, the contribution of z_{KL} was the highest. The telemetry with the highest contribution to z_{KL} was "DIST_SHNT_DRV_V_CAL." Moreover, Figure 9a indicates that its waveform changed significantly.

The contribution of the gradient increasing parts is also shown in Figure 8, indicating that z_{MA} had the highest contribution and that the top five telemetries for contribution to z_{MA} were all related to the battery (BAT). As shown in Figures 9b to 9f, the mean of these telemetries actually changed, where the change in the two current telemetries was slight.

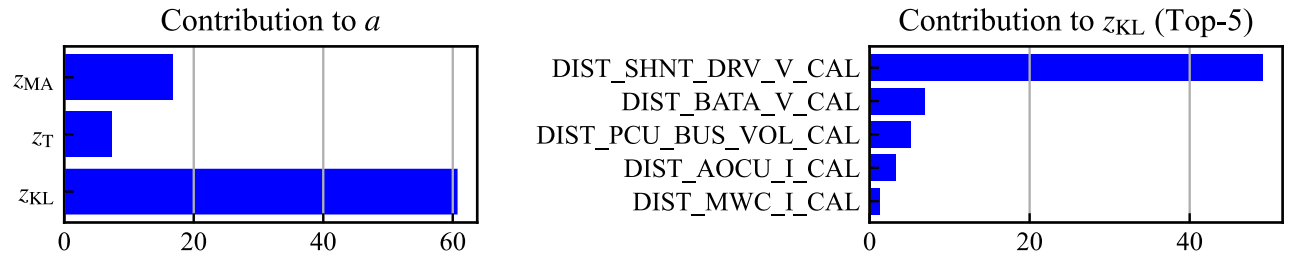

Figure 7. Contributions η to anomaly score and the component of feature vector z_{KL}.

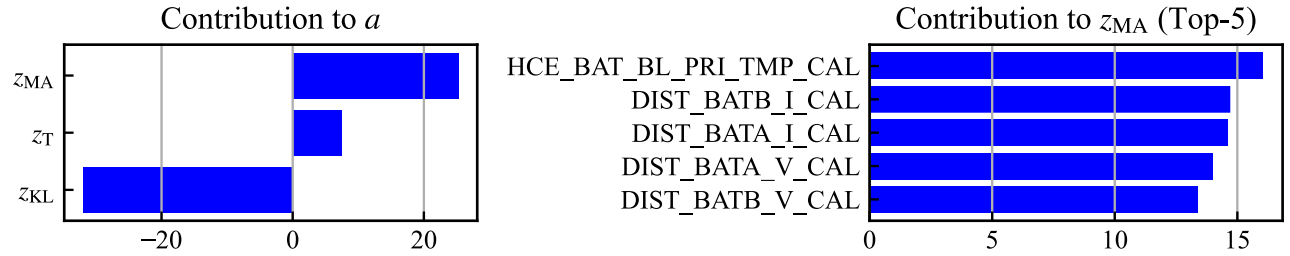

Figure 8. Contributions η to anomaly score and the component of feature vector z_{MA}.

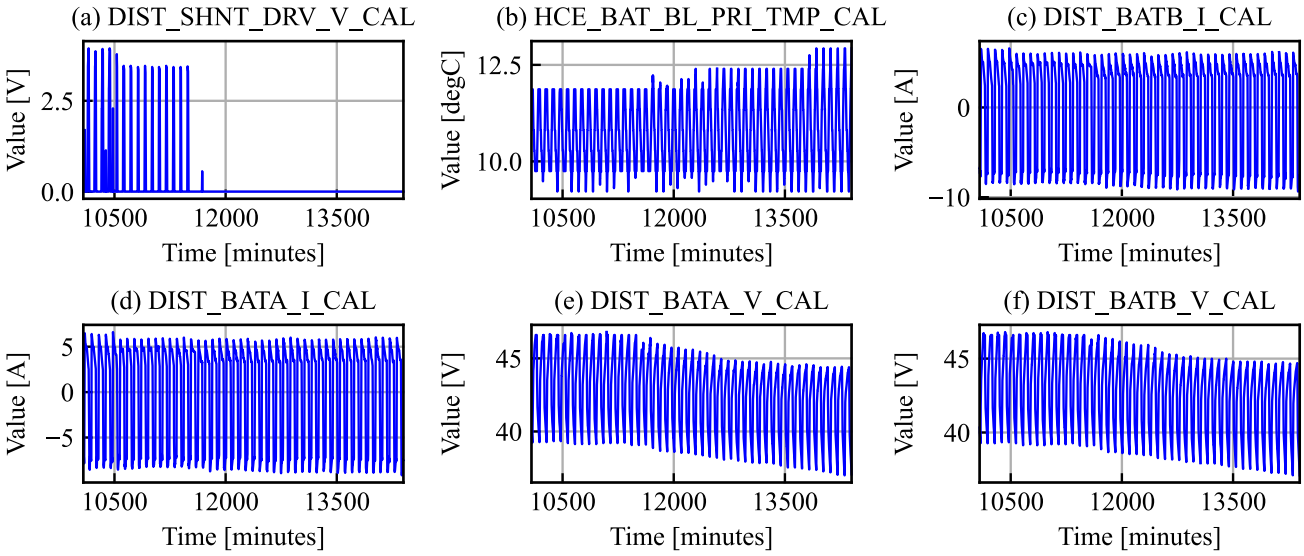

Figure 9. Telemetry with high contribution to the components of feature vector in the practical dataset.

To summarize the above results, what the proposed method provides to operators is that the waveform of the shunt voltage changed abruptly, and the average values of the battery voltage, current, and temperature changed gradually. This information is sufficient for operators to assume that the abnormal event of batteries or power generation has occurred. Therefore, we found that the proposed method can provide useful information to operators in practical operations. Although anomalies such as voltage drops can be detected manually by operators, data-driven automatic detection reduces the burden on operators. In addition, if the proposed method can be implemented on board, downlinking of the features and contributions will enable more comprehensive anomaly detection, considering the telemetry, which could not be downlinked owing to communication capacity limitation.

5. CONCLUSION

In this study, we designed a feature based on the MD and proposed a telemetry monitoring system to assist operators. The proposed method can provide operators with information on the type of anomaly and unusual telemetry

necessary for them to address the anomaly. In the validation phase, we confirmed that it can recognize trend, periodic, and waveform anomalies and identify the telemetry where the anomaly occurred. We also applied it to the anomaly event related to the power system on the actual satellite and showed that it can provide sufficient information for operators to predict and cope with the anomaly.

For future work, different issues could be investigated. First, thresholds are an important issue because they are used to judge the rejection of training data as well as to detect anomalies in the proposed method. It is necessary to set the threshold dynamically because satellite telemetry fluctuates under the influence of equipment degradation and changes in operational mode. Next, in this study, features for trends, periods, and waveforms were extracted using a simple method, but more developed methods need to be adopted to deal with nonperiodic and discrete telemetry. For example, topological data analysis and time-series prediction approaches are effective for detecting changes in waveforms. With future improvements, the proposed method will be a useful telemetry monitoring system that will help improve satellite reliability and reduce the burden on operators.

ACKNOWLEDGMENT

This work was supported by JST SPRING (Grant Number JPMJSP2156). In addition, this study made use of data obtained from Data Archives and Transmission System, provided by the Center for Science-satellite Operation and Data Archive at ISAS/JAXA.

REFERENCES

Barreyre, C., Boussouf, L., Cabon, B., Laurent, B., & Loubes, J.-M. (2019). Statistical methods for outlier detection in space telemetries. In H. Pasquier, C. A. Cruzen, M. Schmidhuber, Y. H. Lee (Eds.), *Space Operations: Inspiring Humankind's Future* (pp. 513-547). Springer, Cham. https://doi.org/10.1007/978-3-030-11536-4_20

Chen, J., Pi, D., Wu, Z., Zhao, X., Pan, Y., & Zhang, Q. (2021). Imbalanced satellite telemetry data anomaly detection model based on bayesian LSTM, *Acta Astronautica, 180*, 232-242. https://doi.org/10.1016/j.actaastro.2020.12.012

Cui, L., Zhang, Q., Shi, Y., Yang, L., Wang, Y., Wang, J., & Bai, C. (2023). A method for satellite time series anomaly detection based on fast-DTW and improved-KNN, *Chinese Journal of Aeronautics, 36*(2), 149-159. https://doi.org/10.1016/j.cja.2022.05.001

Hundman, K., Constantinou, V. Laporte, C., Colwell, I., & Soderstrom, T. (2018). Detecting spacecraft anomalies using LSTMs and nonparametric dynamic thresholding, *Proceedings of the 24th ACM SIGKDD International Conference on Knowledge Discovery & Data Mining*, 387-395. https://doi.org/10.1145/3219819.3219845

Mizutani, M., Hirose, T., Takaki, R., & Honda, H. (2009). ISACS-DOC: monitoring and diagnostic system for AKARI and HINODE, *Transactions of the Japan Society for Aeronautical and Space Sciences, 7*(ists26), Tf_1-Tf_6. https://doi.org/10.2322/tstj.7.Tf_1

Mota-Gutiérrez, C. G., Reséndiz-Flores, E. O., & Reyes-Carlos Y.I. (2018). Mahalanobis-Taguchi system: state of the art, *International Journal of Quality & Reliability Management, 35*(3), 596-613. https://doi.org/10.1108/IJQRM-10-2016-0174

Pilastre, B., Boussouf, L., D'Escrivan, S., & Tourneret, J.-Y. (2020). Anomaly detection in mixed telemetry data using a sparse representation and dictionary learning, *Signal Processing, 168*, 107320. https://doi.org/10.1016/j.sigpro.2019.107320

Ruff, L., Kauffmann, J. R., Vandermeulen, R. A., Montavon, G., Samek, W., Kloft, M., Dietterich, T. G., & Muller, K.-R. (2021). A unifying review of deep and shallow anomaly detection, Proceedings of the IEEE, 109(5), 756-795. https://doi.org/10.1109/JPROC.2021.3052449

Sakurada, M. & Yairi, T. (2014). Anomaly detection using autoencoders with nonlinear dimensionality reduction, *Proceedings of the MLSDA 2014 2nd Workshop on Machine Learning for Sensory Data Analysis*, 4-11. https://doi.org/10.1145/2689746.2689747

Tariq, S., Lee, S., Shin, Y., Lee, M. S., Jung, O., Chung, D., & Woo, S. S. (2019). Detecting anomalies in space using multivariate convolutional LSTM with mixtures of probabilistic PCA, *Proceedings of the 25th ACM SIGKDD International Conference on Knowledge Discovery & Data Mining*, 2123-2133. https://doi.org/10.1145/3292500.3330776

Umezu, R., Sugie, T., Nagase, M., Kokai, R., Takeshima, T., Ebisawa, K., Mitsuda, K., & Yamamoto, Y. (2019). Detection of failure sign of spacecraft using machine learning, *JAXA Research and Development Report: Journal of Space Science Informatics Japan, 8*, 11-20. (in Japanese). https://doi.org/10.20637/JAXA-RR-18-008/0002

Williams, B. C. & Nayak, P. P. (1996). A model-based approach to reactive self-configuring systems, *Proceedings of the AAAI Conference on Artificial Intelligence, 13*, 971-978.

Woodall, W. H., Koudelik, R., Tsui, K.-L., Kim, S. B., Stoumbos, Z. G., & Carvounis, C. P. (2003). A review and analysis of the Mahalanobis—Taguchi system, *Technometrics, 45*(1), 1-15. https://doi.org/10.1198/004017002188618626

Wu, J., Yao, L., Liu, B., Ding, Z., & Zhang, L. (2020). Combining OC-SVMs with LSTM for detecting anomalies in telemetry data with irregular intervals, *IEEE Access, 8*, 106648-106659. https://doi.org/10.1109/ACCESS.2020.3000859

Xiong, L., Ma, H.-D., Fang, H.-Z., Zou, K.-X., & Yi, D.-W. (2011). Anomaly detection of spacecraft based on least squares support vector machine, *2011 Prognostics and*

System Health Management Conference. https://doi.org/10.1109/PHM.2011.5939470

Yairi, T., Takeishi, N., Oda, T., Nakajima, Y., Nishimura, N., & Takata, N. (2017). A data-driven health monitoring method for satellite housekeeping data based on probabilistic clustering and dimensionality reduction, *IEEE Transactions on Aerospace and Electronic Systems, 53*(3), 1384-1401. https://doi.org/10.1109/TAES.2017.2671247

Yairi, T., Fukushima, Y., Liew, C. F., Sakai, Y., & Yamaguchi, Y. (2021). A data-driven approach to anomaly detection and health monitoring for artificial satellites, *Advances in Condition Monitoring and Structural Health Monitoring*, 129-141. https://doi.org/10.1007/978-981-15-9199-0_13

Yepmo, V., Smits, G., & Pivert, O. (2022). Anomaly explanation: a review, *Data & Knowledge Engineering, 137*, 101946. https://doi.org/10.1016/j.datak.2021.101946